Title
Characterization of Adult and Neonatal Articular Cartilage From the Equine Stifle

Authors
White, Jamie L
Salinas, Evelia Y
Link, Jarrett M
et al.

Publication Date
2021

DOI
10.1016/j.jevs.2020.103294

Peer reviewed

Journal of Equine Veterinary Science 96 (2021) 103294

Contents lists available at ScienceDirect

Journal of Equine Veterinary Science

journal homepage: www.j-evs.com

Original Research

Characterization of Adult and Neonatal Articular Cartilage From the Equine Stifle

Jamie L. White [a], Evelia Y. Salinas [b], Jarrett M. Link [b], Jerry C. Hu [b], Kyriacos A. Athanasiou [b,*]

[a] Integrative Pathobiology Graduate Group, University of California, Davis, Davis, CA
[b] Henry Samueli School of Engineering, Department of Biomedical Engineering, University of California, Irvine, Irvine, CA

ARTICLE INFO

Article history:
Received 27 May 2020
Received in revised form
1 October 2020
Accepted 2 October 2020
Available online 15 October 2020

Keywords:
Equine stifle joint
Equine femoropatellar joint
Cartilage characterization
Cartilage tissue engineering
Cartilage mechanical properties

ABSTRACT

A significant portion of equine lameness is localized to the stifle joint. Effective cartilage repair strategies are largely lacking, however, recent advances in surgical techniques, biomaterials, and cellular therapeutics have broadened the clinical strategies of cartilage repair. To date, no studies have been performed directly comparing neonatal and adult articular cartilage from the stifle across multiple sites. An understanding of the differences in properties between the therapeutic target cartilage (i.e., adult cartilage) as well as potential donor cartilage (i.e., neonatal cartilage) could aid in selection of optimal harvest sites within a donor joint as well as evaluation of the success of the grafted cells or tissues within the host. Given the dearth of characterization studies of the equine stifle joint, and in particular neonatal stifle cartilage, the goal of this study was to measure properties of both potential source tissue and host tissue. Articular cartilage of the distal femur and patella (P) was assessed in regards to two specific factors, age of the animal and specific site within the joint. Two age groups were considered: neonatal (<1 week) and adult (4–14 years). Cartilage samples were harvested from 17 sites across the distal femur and patella. It was hypothesized that properties would vary significantly between neonatal and adult horses as well as within age groups on a site-by-site basis. Adult thickness varied by site. With the exception of water content, there were no significant biochemical differences among sites within regions of the distal femur (condyles and trochlea) and the patella in either the adult or neonate. Neonatal cartilage had a significantly higher water content than adult. Surprisingly, biochemical measurements of cellularity did not differ significantly between neonatal and adult, however, adult cartilage had greater variance in cellularity than neonatal. Overall, there were no significant differences between neonatal and adult glycosaminoglycan content. Collagen per wet weight was found to be significantly higher in adult cartilage than neonatal when averaged across all levels. In terms of biomechanical properties, aggregate modulus varied significantly across the condyles of adult cartilage but not the neonate. Neonatal cartilage was significantly less permeable, and the Young's modulus of neonatal cartilage was significantly higher than the adult. The tensile strength did not vary in a statistically significant manner between age groups. An understanding of morphological, histological, biochemical, and biomechanical properties enhances the understanding of cartilage tissue physiology and structure-function relationships. This study revealed important differences in biomechanical and biochemical properties among the 17 sites and among the six joint regions, as well as age-related differences between neonatal and adult cartilage. These location and age-related variations are informative toward determining the donor tissue harvest site.

Animal welfare/ethical statement: All tissues were obtained from cadavers of client-owned horses that had been necropsied at the Veterinary Medical Teaching Hospital, University of California, Davis. The necropsy consent form signed by owners includes an option to opt our research studies.

Conflict of interest statement: There are no known conflicts of interest associated with this manuscript.

* Corresponding author at: Kyriacos A. Athanasiou, Henry Samueli School of Engineering, Department of Biomedical Engineering, University of California, Irvine, 3418 Engineering Hall, Irvine, CA 92697, USA.
E-mail address: athens@uci.edu (K.A. Athanasiou).

https://doi.org/10.1016/j.jevs.2020.103294
0737-0806/

1. Introduction

The stifle joint is notable as the most complex joint in the body. Damage or developmental abnormalities affecting any component of this complex synovial joint can result in lameness and decreased mobility. Lameness associated with the stifle joint has been reported to comprise approximately 40% of hindlimb lameness cases [1]. The articular cartilage lining the ends of the long bones and articulating surface of the patella (P) plays a critical role in proper joint function. In addition to developmental disorders, traumatic injury to the articular cartilage of the stifle joint, underlying the subchondral bone, or soft tissue structures within and surrounding the joint, such as ligaments, menisci, or joint capsule, can also result in osteoarthritis (OA) [2]. The reports of the incidence of OA ranges from 3 to 32% of all stifle lameness that may be attributed to the disease process, with the medial femorotibial joint compartment being the most commonly affected in horses [3]. Effective cartilage repair strategies are largely lacking in both human and veterinary medicine, however, recent advances in surgical techniques, biomaterials, and cellular therapeutics have greatly broadened the clinical strategies of cartilage repair [4–8].

Advanced strategies for cartilage repair include grafting procedures such as the osteochondral allograft transplantation system and mosaicplasty, cellular-based strategies such as autologous chondrocyte implantation (ACI) and matrix-assisted ACI, as well as particulated cartilage–based procedures such as the cartilage autograft implantation system [8]. A handful of these strategies utilize tissue from neonatal and juvenile tissue donor sources, including RevaFlex DeNovo Arthrex Biocartilage, capitalizing on the higher regenerative capacity of chondrocytes from younger donor sources [9]. While a number of these strategies are used routinely in human medicine, they are largely confined to the realm of research in the context of equine medicine. An ideal articular cartilage repair product would result in production of novel hyaline cartilage tissue that recapitulated the zonal architecture and hyaline composition of native articular cartilage and achieve lateral integration into surrounding healthy cartilage and underlying subchondral bone. It is therefore important to understand the properties of native cartilage to establish design criteria for potential therapeutics.

Properties of equine articular cartilage in health have been most extensively characterized in the metacarpophalangeal joint [10–19], however, limited studies have been conducted in other joints such as the carpus [20–25], cervical facet [26], and stifle [27]. To date, no studies have been performed directly comparing neonatal and adult articular cartilage from the stifle on a site-by-site basis. An understanding of the differences between neonatal and adult cartilage can inform theories of the postnatal maturation process, especially when interpreted in conjunction with kinematic/loading force studies. Equine neonatal cartilage may also serve as donor tissue, both as a cell source for tissue engineering efforts as well as a matrix source for allograft procedures [28,29]. An understanding of the differences in properties between the therapeutic target cartilage (i.e., adult cartilage) as well as potential donor cartilage (i.e., neonatal cartilage) could aid in selection of optimal harvest sites within a donor joint as well as evaluation of the success of the grafted cells or tissues within the host.

While a handful of studies have reported properties of the stifle cartilage in the adult equine, most of these studies have only examined compressive and biochemical properties and have only measured properties from a small number of locations across the joint surface. Given the dearth of characterization studies of the equine stifle joint, and in particular neonatal stifle cartilage, the goal of this study was to measure properties of both potential source tissue and host tissue. Articular cartilage of the distal femur and patella was assessed in regards to two specific factors, age of the animal, and location within the joint. It was hypothesized that properties would vary significantly between neonatal and adult horses as well as within age groups by location.

2. Materials and Methods

2.1. Native Tissue Sample Preparation

Equine stifle joints were isolated from six skeletally mature horses (4–14 years old, mean = 6.7 years old) and six neonatal foals (<1 week old). All animals died or were euthanized for reasons unrelated to stifle joint pathology. Stifle joints were harvested within 48 hours of time of death. Animals were stored at 4°C during this interim period of up to 48 hours. Stifle joints were isolated from the animal and stored at −20°C with joint capsule kept intact until time of tissue harvest and testing. Upon opening the stifle joint, a macroscopic inspection of the cartilage was performed to check for any gross abnormalities suggestive of pathology, including OA and osteochondrosis (OC). Horses whose cartilage showed gross signs of OA and OC were excluded from this study. Articular cartilage samples were isolated from the patella and five different regions of the distal femur——the medial condyle (MC), the lateral condyle (LC), the medial ridge of the trochlea (MR), the lateral ridge of the trochlea (LR), and the trochlear groove (TG). Within each of these regions, multiple sites were tested, three sites on MC, three sites on LC, three sites on MR, three sites on LR, three sites on TG, and two sites on P (Fig. 1). Sites were isolated using an 8 mm biopsy punch from the approximate locations detailed in Fig. 1. For adult samples, the cartilage was trimmed off the underlying subchondral bone with a #10 scalpel blade. Neonatal samples were trimmed to ~2 mm thickness (approximate junction between articular cartilage and underlying epiphyseal growth plate cartilage) using a custom jig and microtome blade. Each 8 mm punch was portioned for histologic, biochemical, high-performance liquid chromatography, and biomechanical (compressive and tensile) evaluations (Fig. 1).

2.2. Biomechanical Evaluation

Creep indentation testing was performed on 3 mm cylindrical punches taken from the central portion of the larger 8 mm specimens collected from each region. This 3 mm punch was then photographed using a custom built photography station to ensure consistent distances during photography, and digital measuring tools (ImageJ) were used to determine the thickness at the center of the sample where the indenter tip was applied during testing. The sample was subsequently glued to the base of a cylindrical sample holder and submerged in PBS (Sigma). A 0.9 mm diameter, flat, porous indenter tip was applied to the samples under a 2–12 g load to achieve ~10% strain. The tissue was allowed to reach creep equilibrium while the deformation was recorded over time. Creep deformation data were then used to determine the aggregate modulus, shear modulus, and permeability of each sample using a linear biphasic model [30].

For uniaxial tensile testing, specimens were trimmed into a dog-bone shape with a gauge length of 1.3 mm, in adherence with ASTM International standards (ASTM D3039). Orientation of collagen fibers was determined by pricking the cartilage sample surface with a needle dipped in India ink, which allowed for visualization of a split line running parallel to collagen fiber orientation. Specimens were trimmed such that the long axis of the dog bone was oriented parallel to collagen fiber alignment based on the India ink staining. The samples were photographed to obtain the cross-sectional area of each sample using ImageJ. Paper tabs were glued to the samples outside the gauge length. These tabs were loaded into the grips of a

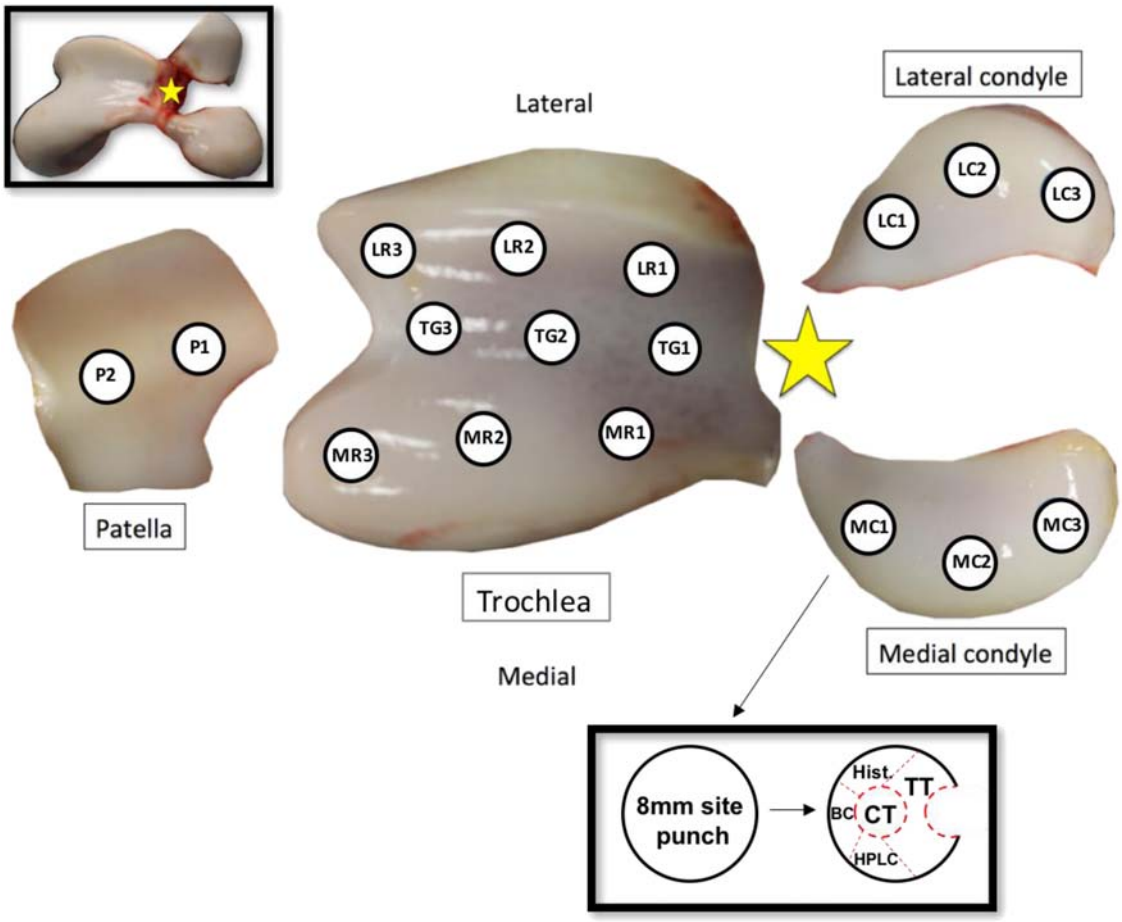

Fig. 1. Articular cartilage from 17 sites across six regions of the distal femur and patella was characterized morphologically, histologically, biochemically, and biomechanically. The inset image at top left shows the distal femur with the star denoting the most axial portion of the joint surface. MC = medial condyle, LC = lateral condyle, LR = lateral ridge of the trochlea, MR = medial ridge of the trochlea, TG = trochlear groove, P = patella. The inset image at bottom right shows how the 8 mm punch from each site was portioned for compression testing (CT), tensile testing (TT), biochemistry (BC), histology (Hist.), and high-performance liquid chromatography (HPLC).

TestResources mechanical tester (TestResources Inc) and pulled at 1% of the gauge length per second until sample failure. Load measurements were recorded over the duration of the test and used to generate stress-stain curves. Young's modulus was obtained by a least-squares fit of the linear region of the curve, and ultimate tensile strength (UTS) was determined from the maximum stress at failure.

2.3. Biochemical Evaluation

Full-thickness samples were portioned from each 8 mm biopsy punch for biochemical analysis including water, collagen, glycosaminoglycan (GAG), and DNA content. The samples were weighed before and after lyophilization to obtain wet weight (WW) and dry weight (DW), respectively. Water content of the tissues was determined using the difference between WW and DW for each sample. The lyophilized samples were digested in 125 μg/mL papain (Sigma) in 50 mM phosphate buffer (pH = 6.5) containing 2 mM N-acetyl cysteine (Sigma) and 2 mM EDTA (Sigma) at 60°C for 18 hours. Sulfated GAG content was measured using the Blyscan dimethyl methylene blue assay kit (Accurate Chemical). Collagen content was quantified by a perchloric acid-free, chloramine-T–modified hydroxyproline assay [31] after hydrolysis with 2 N NaOH for 20 minutes at 110°C, and using Sircol collagen (Accurate Chemical) as a standard. The Quant-iT PicroGreen dsDNA assay kit (Invitrogen) was used to measure the DNA content.

2.4. High-performance Liquid Chromatography

Full-thickness samples were portioned from each 8 mm biopsy punch for high-performance liquid chromatography (HPLC) to quantify pyridinoline cross-link content. For the HPLC assay, the lyophilized samples were digested in 6N HCl at 100°C for 24 hours and then dried in a vacuum concentrator. Digested samples were resuspended in 500 μL of a solution containing 1.67 nmol pyroxidine/mL, 8.3% acetonitrile, and 0.41% heptafluorobutyric acid (HFBA) in water and then injected into a 25 mm C18 column (Shimadzu). Two solvents, (1) 24% methanol and 0.13% HFBA in water and (2) 75% acetonitrile and 0.1% HFBA in water, were sequentially flowed through the column for sample elution and column washing, respectively [32].

2.5. Histologic and Immunohistochemical Evaluation

Full-thickness samples partitioned from the 8 mm punch for histologic processing were fixed in 10% neutral buffered formalin, embedded in paraffin, and sectioned into 4 μm sections to expose the full thickness of the tissue. The sections were stained with Hematoxylin and Eosin (H and E), Safranin O/Fast Green for sulfated GAGs, and Picrosirius red for collagen. Immunohistochemistry (IHC) was performed to visualize collagen type I and collagen type 2. After antigen retrieval with citric acid (pH 6) at 95°C for

20 minutes and at room temperature for an additional 20 minutes, anticollagen I antibody (ab34710, Abcam) was applied at a 1:300 dilution. Antigen retrieval using 4 mg/mL hyaluronidase (Sigma) in PBS for 30 minutes followed by 3 mg/mL pepsin (Sigma) in 0.5% acetic acid for 30 minutes was used before application of anti-collagen II antibody (ab34712, Abcam) at a 1:600 dilution.

2.6. Statistical Analysis

An O'Brien test for unequal variances was performed for all quantitative measures. If variances were unequal, a Welch's test was performed. In the case of equal variances, the analysis was performed by linear mixed model ANOVA treating animal as a random effect followed by Tukey's *post hoc* test. The statistical model included site (1, 2, and 3), region (lateral condyle, medial condyle, lateral trochlear ridge, medial trochlear ridge, trochlear groove, and patella), age (adult vs. neonatal), and the interaction of joint region and age as fixed effects. Data are presented as mean ± standard deviation, and different letters denote significantly different groups at $P < .05$.

3. Results

3.1. Gross Morphology

All animals used in this study had articular cartilage of the femoropatellar joint that appeared healthy, with a smooth, glossy, white appearance. Thickness was measured for all sites in both neonatal and adult cartilage (Table 1). Neonatal cartilage thickness was limited to the depth of the biopsy punch, and, thus, thickness was only measured for the purpose of compressive testing and was not analyzed for significant differences among sites or regions.

The thicknesses of adult cartilage varied significantly among sites within a region (Fig. 2A) and among different regions (Fig. 2B). The thickness of the MC1, MC2, and MC3 sites were 1.51 ± 0.35 mm, 1.80 ± 0.40 mm, and 2.14 ± 0.34 mm, respectively. MC3 was significantly thicker than MC1 and MC2. The thicknesses of the LC1, LC2, and LC3 sites were 1.50 ± 0.51 mm, 0.98 ± 0.21 mm, and 0.75 ± 0.08 mm, respectively. LC1 was significantly thicker than LC3 but not LC2. Interestingly, the thickness increased when moving from cranial to caudal on the medial condyle but decreased when moving from cranial to caudal on the lateral condyle. The thicknesses of the TG1, TG2, and TG3 sites were 1.70 ± 0.23 mm, 1.56 ± 0.30 mm, and 1.60 ± 0.36 mm, respectively. The thicknesses of the MR1, MR2, and MR3 sites were 1.35 ± 0.32 mm, 1.15 ± 0.20 mm, and 1.41 ± 0.38 mm, respectively. The thicknesses of the LR1, LR2, and LR3 sites were 1.95 ± 0.34 mm, 1.78 ± 0.17 mm, and 2.09 ± 0.30 mm, respectively. No significant differences were observed among the three sites for each trochlear region, however, for all trochlear regions the middle site (TG2, MR2, and LR2) was the thinnest site, albeit not significantly thinner than sites 1 and 3. Finally, the thicknesses of the P1 and P2 sites were 1.95 ± 0.28 mm and 1.66 ± 0.35 mm, respectively, and did not differ significantly. In the adult, the overall thicknesses of each region were also compared, and it was determined that the thickness of MC, TG, LR, and P were significantly higher than those of MR and LC. The average thicknesses of MC, LC, TG, MR, LR and P were 1.82 ± 0.44 mm, 1.08 ± 0.44 mm, 1.62 ± 0.29 mm, 1.30 ± 0.31 mm, 1.94 ± 0.29 mm, and 1.80 ± 0.34 mm, respectively.

3.2. Histology

Histologic staining was used to visualize tissue morphology and distribution of sulfated GAG and collagen (Fig. 3). H&E staining of adult articular cartilage revealed that the condyles stained basophilic throughout all zones, whereas trochlear cartilage possessed eosinophilic staining at the surface, and patellar cartilage had an intermediate phenotype that was more basophilic than trochlear cartilage but less basophilic than condylar cartilage. In neonatal articular cartilage, this phenotype was reversed, with the condyles showing less basophilic staining than the trochlea and P. Overall, neonatal cartilage appeared more homogeneous and more cellular, however, cell lacunae were more pronounced in adult cartilage. Safranin-O (with a fast green counterstain) was used to visualize

Table 1
Thickness, hydration, and cross-links per collagen of neonatal and adult articular cartilage from specific regions and sites within each region.

Location	Adult	Neonatal	Adult	Neonatal	Adult
	Thickness (mm)	Hydration (%)		HPLC/Col (ug/ug)	
Medial condyle (MC)					
1	1.51 ± 0.35	80.33 ± 1.75	78.00 ± 2.10	0.33 ± 0.33	0.19 ± 0.22
2	1.80 ± 0.40	80.20 ± 3.35	81.33 ± 1.51	0.10 ± 0.10	0.60 ± 0.45
3	2.14 ± 0.34	77.57 ± 2.07	80.67 ± 2.58	0.14 ± 0.12	0.48 ± 0.59
Lateral condyle (LC)					
1	1.50 ± 0.51	77.33 ± 0.75	78.33 ± 0.82	0.06 ± 0.03	0.40 ± 0.38
2	0.98 ± 0.21	80.00 ± 1.67	79.17 ± 1.47	0.09 ± 0.08	0.40 ± 0.42
3	0.75 ± 0.08	81.00 ± 0.75	80.33 ± 1.21	0.05 ± 0.02	0.45 ± 0.51
Trochlear groove (TG)					
1	1.70 ± 0.23	79.83 ± 2.50	78.00 ± 1.22	0.07 ± 0.08	0.65 ± 0.40
2	1.56 ± 0.30	81.50 ± 1.67	78.00 ± 2.61	0.05 ± 0.02	0.52 ± 0.53
3	1.60 ± 0.36	81.83 ± 1.55	76.83 ± 0.98	0.19 ± 0.32	0.54 ± 0.46
Medial ridge (MR)					
1	1.35 ± 0.32	83.33 ± 2.42	76.50 ± 1.05	0.04 ± 0.06	0.55 ± 0.48
2	1.15 ± 0.20	82.50 ± 3.35	78.17 ± 1.60	0.02 ± 0.01	0.20 ± 0.30
3	1.41 ± 0.38	81.83 ± 2.07	77.17 ± 1.47	0.06 ± 0.05	0.40 ± 0.48
Lateral ridge (LR)					
1	1.95 ± 0.34	81.67 ± 1.52	77.83 ± 0.75	0.06 ± 0.07	0.56 ± 0.49
2	1.78 ± 0.17	82.67 ± 1.75	78.33 ± 0.82	0.07 ± 0.07	0.57 ± 0.42
3	2.09 ± 0.30	81.83 ± 1.63	78.50 ± 1.52	0.11 ± 0.11	0.34 ± 0.38
Patella (P)					
1	1.95 ± 0.28	80.50 ± 1.37	77.33 ± 1.21	0.07 ± 0.03	0.32 ± 0.34
2	1.66 ± 0.35	82.33 ± 1.17	78.17 ± 0.41	0.06 ± 0.07	0.39 ± 0.33

Data are presented as mean ± s.d. Thickness of neonatal cartilage is not presented as neonatal cartilage thickness was limited to the depth of the punch and was only measured for the purposes of mechanical testing.

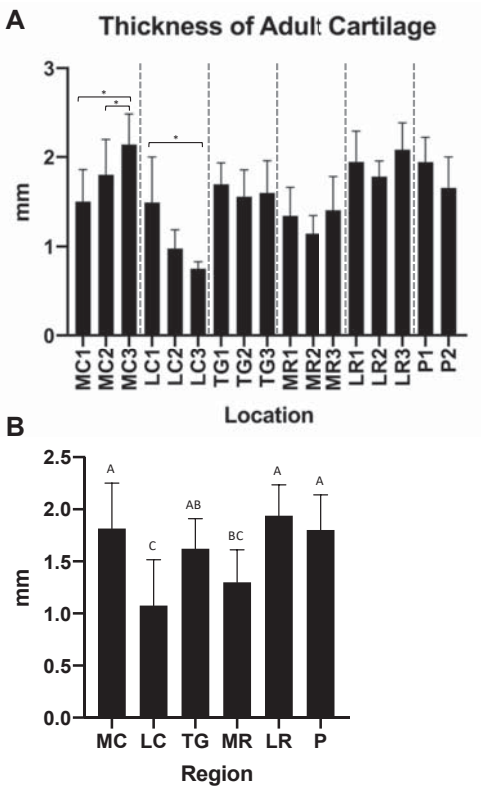

Fig. 2. Thickness of adult articular cartilage. All values are presented as mean ± s.d. Thickness of neonatal cartilage was not assessed as the subchondral bone is not completely mineralized in neonates. A) Average thickness at all sampled sites across the joint. Each region is denoted by dashed gray vertical bars. Sites were compared within each region, and starred bars (*) represent significant differences among sites within an individual region. MC3 is thicker than MC1 and MC2, whereas LC1 is significantly thicker than LC3. B) Average thickness across sites within each region. Regions that share the same letter above the error bars do not differ significantly. MC, TG, LR, and P are thicker than LC and MC, LR, and P are thicker than MR.

sulfated GAG distribution. In both neonatal and adult cartilage, stain intensity was generally highest in the deep zone. In many regions of adult cartilage, staining was faint or absent in the most superficial region. This is likely an artifact of tissue processing, however, it suggests that this region may contain less GAG in adult cartilage compared with neonatal cartilage. A picrosirius red stain was used to visualize collagen distribution. Adult cartilage generally had higher staining intensity than neonatal cartilage, and in many cases, staining was more intense in the superficial zone. Immunohistochemistry for type I and II collaged showed consistently strong collagen II staining and faint collagen I staining for both adult and neonatal cartilages across all sites (Fig. 4).

3.3. Biochemical Properties

The biochemical content of articular cartilage in the different sites for each age group is shown in Tables 1 and 2. With the exception of water content, there were no significant biochemical differences among sites 1, 2, and 3 for each region (MC, LC, TG, MR, LR, and P) in either the adult or neonate. In the adult, the water content of M1 was significantly greater than that of M2, whereas in the neonate, the water content of M3 was significantly less than M2 and M1, and L1 was significantly less than L3. Averaging across all sites, the water content of neonatal and adult cartilage differed significantly with a mean water content of 80.98 ± 1.33% and 78.36 ± 1.06%, respectively. The variability in water content in neonatal cartilage was also significantly greater than adult cartilage. Comparing different regions within the neonatal cartilage revealed that MR, LR, and P had significantly higher water content than both condyles, whereas in adult, the lateral and medial condyles had the highest water content (Fig. 5A).

Collagen cross-linking was measured on a per collagen weight basis. There were no significant differences in collagen cross-linking between age groups or among sites and regions. Cross-linking trended higher in adult cartilage, however, the difference in average cross-link content between adult and neonatal cartilage was not statistically significant. Cross-link content in the adult had greater variance among regions than neonatal cartilage (Fig. 5B).

There were no significant differences between neonatal and adult GAG/WW or GAG/DW, nor were there any significant differences among regions in neonatal cartilage. Adult cartilage, however, did differ significantly among regions with LC having significantly greater GAG/WW and GAG/DW than TG and MC. Interestingly, MC had the lowest GAG content in both adult and neonatal cartilage. GAG/WW averaged 2.86 ± 0.32% and 3.44 ± 0.60% in the neonate and adult, respectively. GAG/DW averaged 15.16 ± 2.20% 16.05 ± 2.70% in neonatal and adult, respectively (Figs. 5C and 5D).

In regards to collagen content, Col/WW varied significantly between neonatal and adult cartilage when averaged across all levels at 10.61 ± 2.23% and 13.80 ± 1.54%, respectively. Col/DW, however, did not, with neonatal cartilage possessing 57.50 ± 14.24% and adult possessing 64.69 ± 9.27%. In the neonate, the regions of the trochlea had the highest collagen content, whereas in the adult, the condyles had the highest collagen content (Figs. 5E and 5F).

Cellularity did not differ significantly between neonatal and adult, however, adult cartilage had greater variability in cellularity than neonatal. Making the assumption of 7.7 pg of DNA per cell [33], the cells/WW and cells/DW were calculated and averaged 18,631 ± 1,720 cells/mg and 99,830 ± 12,674 cells/mg, respectively, in the neonate and 24,209 ± 8,466 cells/mg and 112,706 ± 43,074 cells/mg, respectively, in the adult. Also in the adult, the lateral condyle had significantly greater cellularity than all other regions (Figs. 5G and 5H).

3.4. Biomechanical Properties

The biomechanical properties at the different sites for each age group are shown in Tables 3 and 4. In regards to compressive properties, aggregate modulus varied significantly among sites 1, 2, and 3 in MC and LC of adult cartilage but not neonatal. In the adult, LC1 had a significantly higher aggregate modulus than LC3, and both MC1 and MC2 were significantly higher than MC3. Comparing adult and neonatal compressive properties revealed that adult aggregate modulus had a significantly greater amount of variability than neonatal, and neonatal cartilage possessed on average a significantly higher aggregate modulus with an average of 354 ± 43 kPa than the adult with an average of 282 ± 47 kPa. There were no significant differences among regions in the neonate, but in the adult, P was significantly higher than MC (Fig. 6A).

Shear moduli also varied significantly among sites 1, 2, and 3 in the adult only, with site 1 significantly higher than site 3 for both MC and LC. There was no significant difference between the overall shear modulus of neonatal and adult cartilage, which were 216 ± 28 kPa and 155 ± 24 kPa, respectively, nor were there significant differences among regions in either age group (Fig. 6B).

Permeability of adult cartilage had greater variance than neonatal cartilage and also significantly higher on average. Neonatal cartilage had an average permeability of 3.26 ± 0.41 $m^4 \times 10^{-15}$/N.s, whereas adult cartilage had an average permeability of 5.09 ± 0.66 $m^4 \times 10^{-15}$/N.s. In the adult, permeability varied

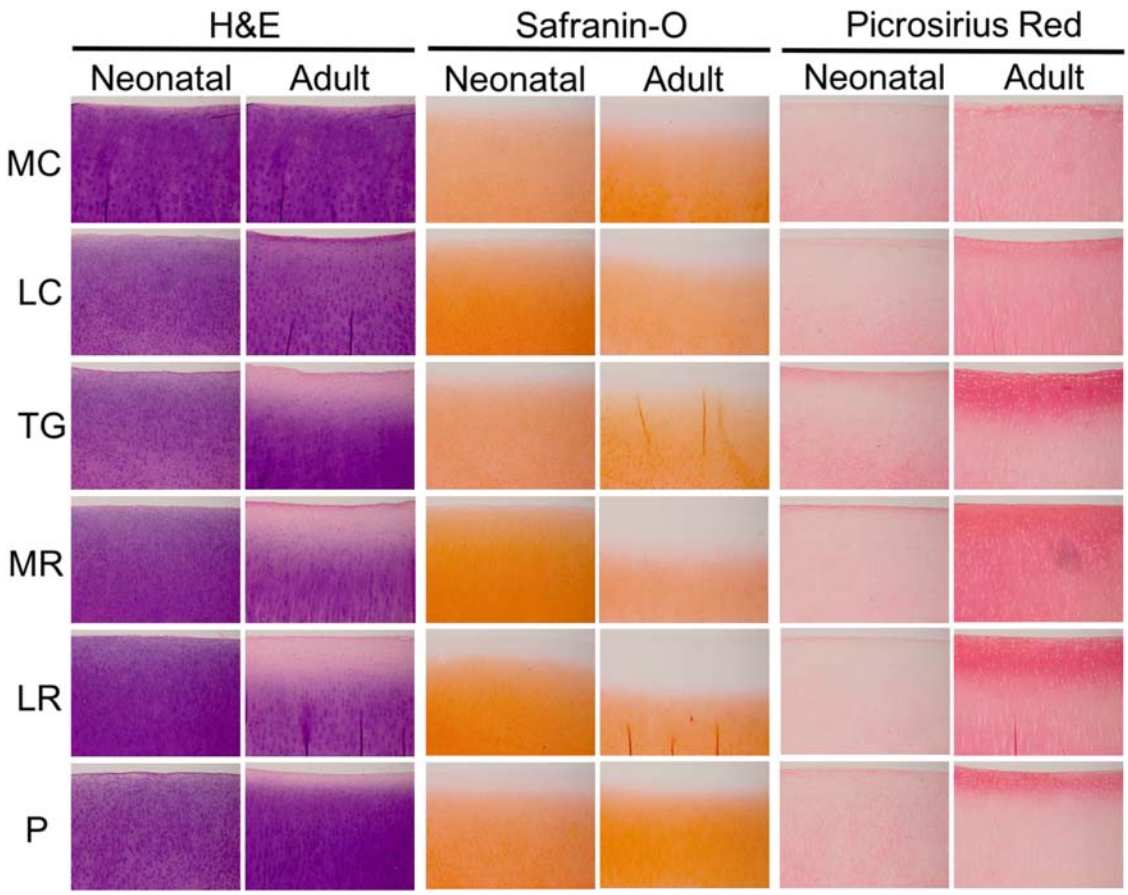

Fig. 3. Histologic evaluation of neonatal and adult articular cartilage cross sections from site 2 of each region. Neonatal cartilage stained more homogeneously basophilic with H&E stain as compared to adult cartilage. Adult cartilage stained eosinophilic in the superficial zone of the trochlear and patellar samples with H&E. Safranin-O stain for GAG was distributed through a greater proportion of neonatal cartilage compared to adult cartilage. Picrosirius red stain for collagen was more intense in adult cartilage compared to neonatal, particularly in the superficial zone.

significantly among sites on the MC, with MC1 being significantly more permeable than both MC2 and MC3 (Fig. 6C).

In regards to tensile properties, there were no significant difference among sites 1, 2, and 3 in either the neonatal or adult. The Young's modulus of neonatal cartilage demonstrated greater variance than the adult and was also significantly higher on average. Neonatal cartilage had a Young's modulus of 16.2 ± 3.9 MPa, and adult cartilage had a Young's modulus of 9.6 ± 2.1 MPa, on average. In the neonate, the Young's modulus of MR was significantly lower than the condyles and TG (Fig. 7A). The UTS did not vary significantly between age groups. In the neonate, however, TG had a significantly higher UTS than MR and LR (Fig. 7B).

4. Discussion

Despite its role as the most complex joint in the horse, the stifle joint is largely understudied in terms of its articular cartilage properties. Injury to the stifle joint is common in the equine athlete, and repair strategies are lacking. Neonatal cartilage offers a potential source for both allogeneic tissue grafts or chondrocytes that may be used to generate repair tissue *in vitro* or *in vivo*. The purpose of this study, therefore, was to characterize the morphological, histological, biochemical, and biomechanical properties of the distal femur and patella in both neonatal and adult horses across the topography of the joint surface. It was hypothesized that these properties would vary between neonatal and adult horses as well as among locations within each age group. The hypothesis was confirmed as significant differences were found between adult and neonatal cartilage and among sites and regions within each age group in regards to morphologic and histologic features, as well as biochemical and biomechanical properties.

In terms of morphology, thickness of adult cartilage was analyzed in this study for variability across sites. Variability in thickness was most pronounced in the condylar regions: MC3 was significantly thicker than MC1 and MC2, whereas LC1 was significantly thicker than LC3 but not LC2. This pattern of increasing thickness of the medial condyle and decreasing thickness of the lateral condyle while moving from cranial to caudal across each condylar surface is consistent with a previous study that topographically examined cartilage thickness of the equine distal femur [27]. The thinner areas of each condyle (the cranial aspect of the medial condyle and caudal aspect of the lateral condyle) correspond to areas that have been demonstrated to experience the greatest amount of contact with underlying meniscal tissue [34], supporting the theory that cartilage thickness may be influenced by mechanical forces [17,35].

Similar to thickness, compressive biomechanical properties and aggregate and shear moduli varied significantly among sites 1, 2, and 3 of the MC and LC of adult cartilage. This variability was not observed in neonatal cartilage. While neonatal cartilage possessed on average a significantly higher aggregate modulus, adult aggregate modulus had a significantly greater amount of variability across locations than neonatal cartilage. This finding is consistent with a study comparing biomechanical properties of cartilage in

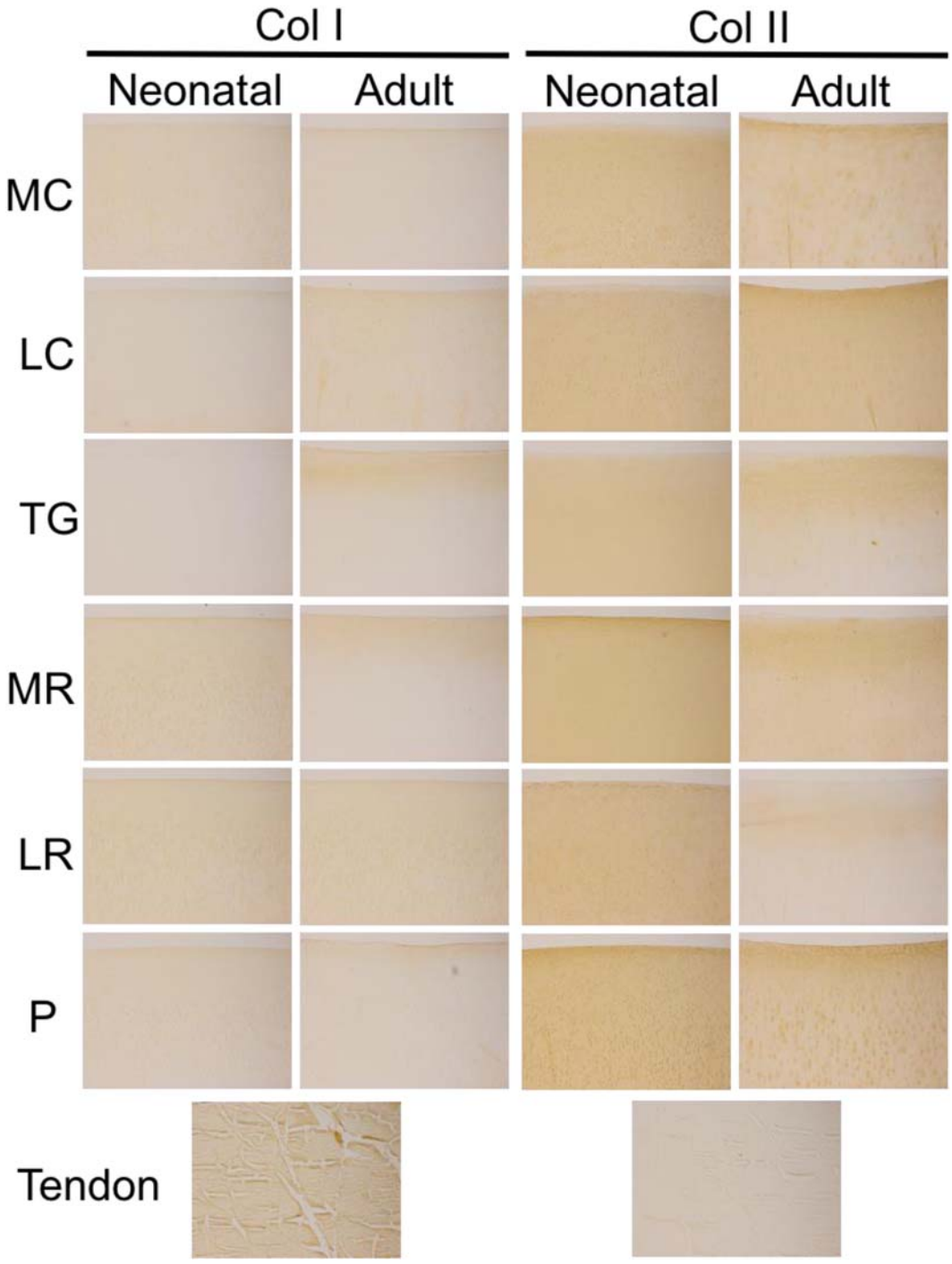

Fig. 4. Immunohistochemical evaluation of neonatal and adult articular cartilage from site 2 of each region. Tendon, which is primarily composed of collagen I, served as control. Both adult and neonatal cartilage stained more intensely for collagen II as compared with collagen I, whereas tendon stained more intensely for collagen I compared with collagen II. Overall, there were no dramatic differences between neonatal and adult cartilage in terms of specific collagen content staining using immunohistochemistry.

fetal, juvenile, and adult equine cartilage at multiple sites, which found that fetal and juvenile cartilage possessed higher compressive properties than adult cartilage but did not vary significantly among sites [17]. The results of this study are also consistent with a previous topographical study of the equine stifle, which found higher compressive properties at the cranial aspect of the condyles in adult horses [27]. Kinematic analysis of the equine stifle demonstrated that cranial and central area of the condyles corresponded with higher articular contact intensity than the more caudal aspect of the condyles [36]. These regions of increased contact intensity correspond with regions of higher compressive properties in the adult but not the neonate, further supporting the concept of a functional adaptation process in response to physiologic loading.

Interestingly, in the adult, the MC region had both the lowest compressive and tensile properties than all other regions. In a relatively small study of 47 horses, lesions in the medial femoral condyle and medial meniscus were more prevalent compared with

Table 2
GAG, collagen, and cell number on a per wet weight (WW) and per dry weight (DW) basis of neonatal and adult articular cartilage from specific regions and sites within each region.

Location	Neonatal		Adult		Neonatal		Adult		Neonatal		Adult	
	GAG/WW (%)	GAG/DW (%)	GAG/WW (%)	GAG/DW (%)	Col/WW (%)	Col/DW (%)	Col/WW (%)	Col/DW (%)	Cell #/WW	Cell #/DW	Cell #/WW	Cell #/DW
Medial condyle (MC)												
1	2.33 ± 0.63	12.12 ± 6.55	3.17 ± 1.17	13.50 ± 3.62	6.67 ± 14.18	34.67 ± 19.03	16.17 ± 4.96	74.00 ± 21.20	19438 ± 7899	99897 ± 31054	22999 ± 13676	104887 ± 62547
2	2.80 ± 1.47	13.00 ± 8.49	2.50 + 1.38	13.83 ± 6.11	9.00 ± 1.22	57.00 ± 21.70	13.17 ± 2.79	68.00 ± 2.38	20518 ± 6417	115661 ± 47423	12119 ± 6846	62445 ± 34672
3	2.57 ± 1.26	11.14 ± 3.18	2.17 ± 0.98	11.00 ± 5.59	7.71 ± 1.80	33.43 ± 7.91	13.67 ± 2.66	69.83 ± 11.97	17330 ± 7519	79692 ± 45869	15005 ± 6967	78300 ± 55154
Lateral condyle (LC)												
1	2.33 ± 1.17	10.83 ± 5.53	4.50 ± 1.05	19.83 ± 4.36	11.67 ± 1.62	54.00 ± 10.53	16.33 ± 1.75	75.00 ± 8.85	17186 ± 9244	81223 ± 44140	37912 ± 7211	175210 ± 103385
2	3.00 ± 1.51	15.83 ± 7.41	4.83 ± 1.94	22.33 ± 7.47	11.20 ± 1.92	55.40 ± 9.10	18.67 ± 6.86	87.83 ± 30.93	17884 ± 7535	87071 ± 30094	51355 ± 20022	201229 ± 124836
3	2.83 ± 1.51	13.83 ± 2.79	3.83 ± .0.98	20.17 ± 4.88	8.67 ± 2.58	42.83 ± 12.06	13.20 ± 2.59	75.83 ± 24.59	15744 ± 8448	78426 ± 43025	32283 ± 8507	217376 ± 133904
Trochlear groove (TG)												
1	3.17 ± 1.37	16.00 ± 5.06	3.33 ± 82	16.50 ± 5.24	15.17 ± 4.67	77.67 ± 24.97	11.33 ± 3.83	54.33 ± 20.75	15221 ± 7668	78098 ± 37127	11896 ± 7211	57553 ± 32795
2	2.67 ± 1.10	15.33 ± 8.55	2.83 ± 75	14.33 ± 4.08	9.83 ± 3.54	55.33 ± 21.15	10.83 ± 3.54	49.67 ± 11.06	15975 ± 7124	86629 ± 37499	13830 ± 8104	64791 ± 3441
3	2.33 ± 0.75	13.50 ± 8.46	3.17 ± 1.47	14.00 ± 6.90	13.00 ± 3.41	73.00 ± 18.37	11.83 ± 1.94	52.17 ± 9.89	17664 ± 8043	97495 ± 45014	30442 ± 21973	131066 ± 90432
Medial ridge (MR)												
1	3.00 ± 1.75	17.50 ± 5.68	3.50 ± 0.55	15.00 ± 3.52	12.17 ± 3.43	75.33 ± 23.01	13.50 ± 2.43	57.33 ± 10.11	16919 ± 7899	104931 ± 50480	28512 ± 11231	121703 ± 46462
2	2.83 ± 1.92	16.00 ± 5.66	4.00 ± 1.26	17.17 ± 5.71	12.00 ± 4.77	68.67 ± 28.32	12.50 ± 3.83	59.17 ± 16.62	17211 ± 9277	23163 ± 8873	25280 ± 16556	116364 ± 72597
3	2.00 ± 0.79	12.00 ± 6.45	3.33 ± 1.37	15.83 ± 5.98	17.17 ± 4.12	97.33 ± 26.86	14.33 ± 3.44	62.67 ± 15.63	97576 ± 47413	129168 ± 45869	17374 ± 6967	74565 ± 28750
Lateral ridge (LR)												
1	3.50 ± 0.98	17.50 ± 3.39	3.50 ± 1.22	15.8 ± 4.31	9.67 ± 3.67	50.83 ± 17.17	11.33 ± 3.20	49.67 ± 14.56	15580 ± 7191	83247 ± 35566	20050 ± 17212	88966 ± 76922
2	3.33 ± 0.82	19.83 ± 6.49	4.00 ± 1.79	19.00 ± 8.02	10.33 ± 3.50	59.33 ± 17.19	13.67 ± 6.50	64.33 ± 31.11	19387 ± 8238	113977 ± 49940	23565 ± 17936	107395 ± 78804
3	3.00 ± 0.55	14.83 ± 7.99	3.50 ± 0.55	16.00 ± 2.19	8.50 ± 2.51	46.83 ± 14.81	15.33 ± 2.73	71.67 ± 13.03	23282 ± 9342	127229 ± 50080	27729 ± 13210	128023 ± 61199
Patella (P)												
1	2.83 ± 1.21	15.17 ± 4.67	3.17 ± 1.17	14.33 ± 4.80	9.50 ± 3.21	48.83 ± 13.41	15.33 ± 3.93	69.50 ± 17.69	19214 ± 8540	97807 ± 39406	17374 ± 12545	77906 ± 55193
2	3.67 ± 1.55	20.50 ± 4.59	3.33 ± 0.52	15.33 ± 1.97	9.33 ± 2.50	53.33 ± 17.80	13.001 2.00	59.17 ± 9.50	22687 ± 9066	126603 ± 43078	26320 ± 18516	121318 ± 84902

Data are presented as mean ± s.d.

the lateral condyle and meniscus [37]. The cranial pole of the medial meniscus undergoes less cranial-caudal translation and higher axial compressive strain than the lateral meniscus during physiologic loading [38]. The forces required to generate this meniscal strain on the cranial pole of the medial meniscus are primarily transmitted through the cranial and central aspect of the medial femoral condyle during locomotion and correspond with areas of higher compressive properties within the medial condyle. Over time, the high strain experience by the medial condyle may result in accelerated wear to the cartilage in this joint compartment and may explain the lower biomechanical properties measured in this region.

Measurements of cellularity did not differ significantly between the neonate and adult, however, adult cartilage had greater variance in cellularity with neonatal cartilage. Upon histologic examination, neonatal cartilage appeared more homogeneous and more cellular compared with adult cartilage. Studies of the equine fetlock joint in the adult have demonstrated variations in DNA content as great as 1.7-fold across this joint surface [13]. In this study, cellular content varied up to 1.9-fold in the adult equine stifle, with areas of higher cell content corresponding to areas with higher GAG content. This correlation between cellularity and GAG content was not found in neonatal cartilage, however. In general, cellularity of cartilage is thought to decrease with age, so the finding in this study of similar cellular content in both age groups was unexpected. Cellularity was determined by measuring DNA content and calculating cell number based on the assumption that most mammalian cells contain approximately 7.7 pg of DNA per cell [33]. This study measuring DNA quantity was performed in adult rat cells, and it is uncertain whether neonatal cells also contain comparable levels of DNA. Other studies of human, rat, frog, crustacean, and plant cells have shown increases in cell volume correlate strongly with increases in nuclear DNA mass [39]. Histologically, the neonatal chondrocytes appear to be smaller than the adult chondrocytes, and therefore may contain less nuclear DNA. This suggests that assuming neonatal and adult equine chondrocytes have 7.7 pg of DNA per cell may be an oversimplification and could inflate the number of adult chondrocytes compared with neonatal chondrocytes. Another potential explanation for the relatively high cellularity of adult cartilage in this study is that there may have been some early degenerative changes in the samples tested that were not detected upon gross examination, as one of the early changes in OA is an increase in cellularity as well as GAG content [40,41].

Histologic staining also revealed that GAG distribution in both neonatal and adult cartilage was generally highest in the deep zone, and the superficial zone contained less GAG in adult cartilage compared with neonatal cartilage. This variation in GAG content corresponding with cartilage depth has also been observed in the equine fetlock [42]. Moreover, similar to fetlock cartilage, the degree of GAG variability across cartilage depth is higher in adult cartilage than neonatal cartilage [42]. Biochemical assays revealed that the MC region had the lowest GAG content in both adult and neonatal cartilage, although, overall, there were no significant differences between neonatal and adult GAG content. This lower GAG content in the MC in the adult may explain lower compressive properties observed in the adult in this region, as GAG content has been shown to correlate positively with compressive properties [43].

Adult cartilage generally had higher collagen staining than neonatal cartilage, and in many cases, staining was more intense in the superficial zone. Supporting this histologic observation, Col/WW was found to be significantly higher in adult cartilage than neonatal when averaged across all regions. This

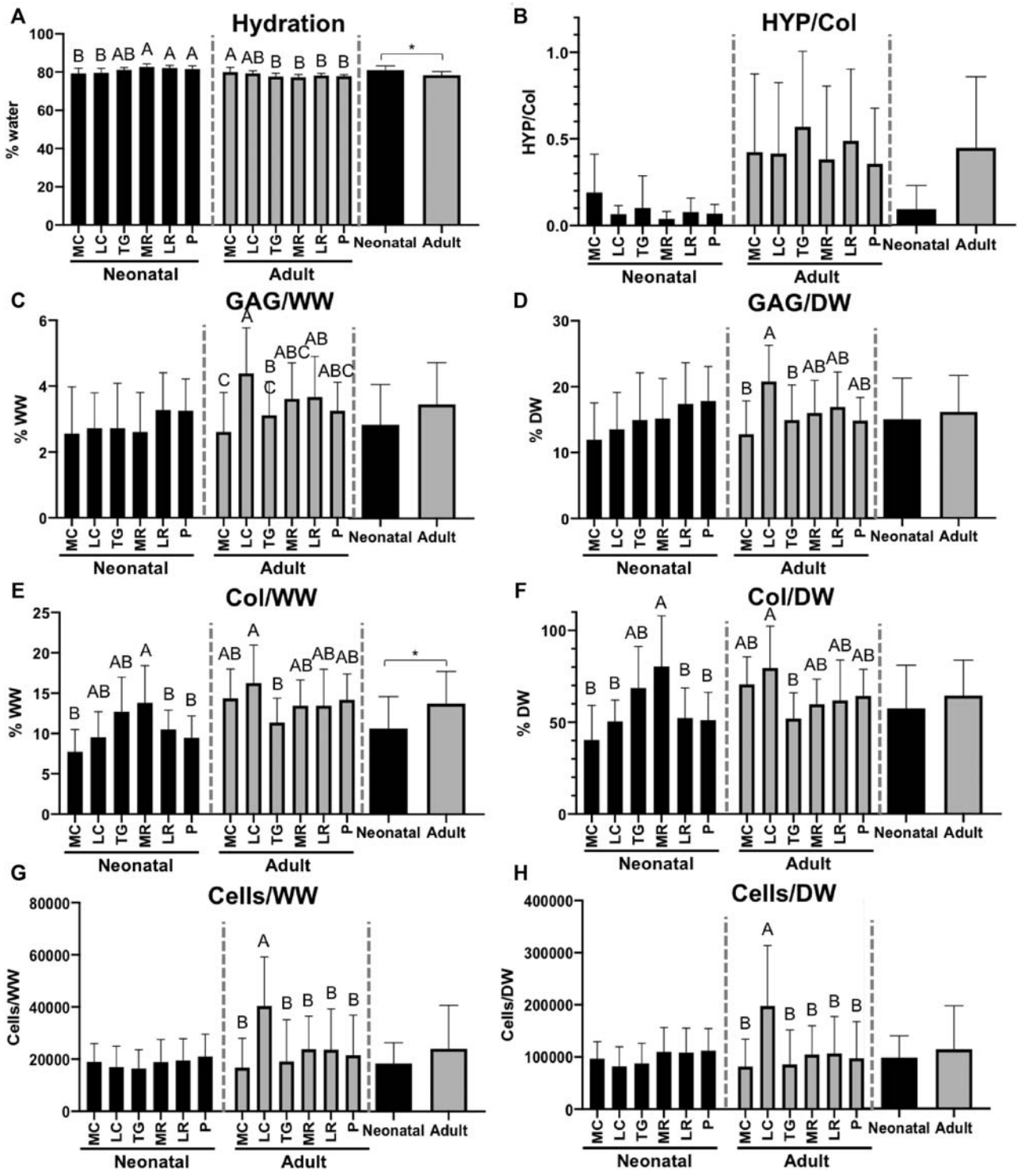

Fig. 5. Biochemical characterization of regions and overall average for each age group: neonatal and adult. All values are presented as mean ± s.d. Starred bars (*) represent significant differences between age groups while regions that do not share the same letter within each age group differ significantly. (A) Hydration varied among regions in both the neonate and adult, and there was a significant difference of overall hydration between age groups. (B) Collagen cross-linking (HYP) on a per collagen weight basis did not vary significantly among regions or between age groups, however, there was a trend for greater cross-linking in the adult. GAG varied among regions in the adult on a per wet weight (WW) (C) and per dry weight (DW) (D) basis. Collagen varied among regions in both the neonate and the adult on a per WW (E) and per DW (F) basis. In addition, collagen/WW differed overall between the neonate and adult (E). Cellularity varied among regions in the adult on a per WW (G) and per DW (H) basis but did not vary overall between the neonate and the adult. Biochemical data are available in Tables 1 and 2

Table 3
Compressive properties of neonatal and adult articular cartilage from specific regions and sites within each region.

Location	Neonatal			Adult		
	Aggregate Modulus (kPa)	Shear Modulus (kPa)	Permeability ($m^4 \times 10^{15}$/N.s)	Aggregate Modulus (kPa)	Shear Modulus (kPa)	Permeability ($m^4 \times 10^{15}$/N.s)
Medial condyle (MC)						
1	356 ± 53	192 ± 62	3.07 ± 1.26	**307 ± 82^{A}**	**173 ± 79^{A}**	**2.9 ± 0.84^{A}**
2	406 ± 110	252 ± 75	2.61 ± 1.02	**370 ± 96^{A}**	**157 ± 86^{A}**	**2.95 ± .65^{A}**
3	448 ± 169	277 ± 67	3.01 ± 1.34	**81 ± 42^{B}**	**35 ± 56^{B}**	**11.00 ± 4.78″**
Lateral condyle (LC)						
1	334 ± 120	199 ± 70	2.87 ± 0.84	**410 ± 162^{A}**	**241 ± 69^{A}**	5.12 ± 2.46
2	309 ± 38	199 ± 33	2.69 ± 0.84	270 ± 161	184 ± 72	5.80 ± 3.05
3	299 ± 59	182 ± 31	2.92 ± 0.62	**204 ± 54^{B}**	**71 ± 68^{B}**	5.13 ± 0.80
Trochlear groove (TG)						
1	342 ± 86	204 ± 47	3.26 ± 1.57	204 ± 115	120 ± 103	5.80 ± 3.12
2	297 ± 105	169 ± 61	2.63 ± 0,88	307 ± 186	142 ± 137	6.40 ± 3.39
3	289 ± 76	174 ± 50	3.36 ± 1.40	370 ± 171	185 ± 15	4.66 ± 2.10
Medial ridge (MR)						
1	284 ± 53	172 ± 33	3.30 ± 1,45	231 ± 128	132 ± 46	5.42 ± 3.86
2	320 ± 110	195 ± 74	3.40 ± 1.66	220 ± 148	131 ± 60	4.73 ± 1.68
3	372 ± 169	233 ± 101	3.38 ± 1.60	315 ± 95	177 ± 15	6.03 ± 3.78
Lateral ridge (LR)						
1	394 ± 118	267 ± 88	4.45 ± 3.79	208 ± 120	107 ± 80	4.03 ± 2.87
2	372 ± 134	204 ± 46	3.09 ± 1,08	295 ± 108	161 ± 52	4.20 ± 2.94
3	358 ± 118	219 ± 74	2.88 ± 1.04	369 ± 149	198 ± 64	3.72 ± 2.12
Patella (P)						
1	394 ± 118	267 ± 88	4.45 ± 3.79	445 ± 156	244 ± 60	4.84 ± 2.27
2	401 ± 119	234 ± 62	3.38 ± 2.25	272 ± 95	146 ± 80	4.30 ± 1.77

Data are presented as mean ± s.d. Sites that varied significantly within a region are bolded with a superscript letter; sites with unique superscript letters varied significantly. Properties that varied significantly between adult and neonatal cartilage when averaged across all sites are highlighted in dark gray.

phenomenon of higher collagen content in the superficial zone of adult equine cartilage than neonatal equine cartilage has also been previously observed in the fetlock joint [42]. In the neonatal stifle joint, the regions of the trochlea had the highest collagen content, whereas in the adult, the condyles had the highest collagen content. Collagen cross-linking trended higher in adult cartilage and had greater variance than neonatal cartilage. This increase in cross-linking as well as overall collagen content is similar to that observed previously in a study comparing neonatal cartilage and cartilage from yearling horses [19].

While collagen content and cross-linking generally correlate positively with tensile properties [43], surprisingly, the stiffness (Young's modulus) of neonatal cartilage was significantly higher on average in the neonate than the adult. In the neonate, the Young's modulus of MR was significantly lower than the condyles and TG. Cartilage tensile strength (UTS) did not vary significantly between

Table 4
Tensile properties of neonatal and adult articular cartilage from specific regions and sites within each region.

Location	Neonatal		Adult				
	Young's Modulus (MPa)	UTS (MPa)	Young's Modulus (MPa)		UTS (MPa)		
Medial condyle (MC)							
1	14.0 ± 4.1	6.6 ± 3.7	10.9 ± 6.2		4.9 ± 2.3		
2	17 ± 5.9	7.5 ± 3.6	4.1 ± 2.4	A	2.0 ± 1.7		AB
3	22.4 ± 10.7	7.0 ± 3.9	2.4 + 1.1		3.7 ± 4.7		
Lateral condyle (LC)							
1	21.2 ± 8.9	6.2 ± 2.5	12.5 ± 11.2		5.8 ± 3.5		
2	16.4 ± 8.9	6.2 ± 3.7	9.1 ± 3.1	A	5.3 ± 1.8		AB
3	18.4 ± 10.9	8.2 ± 3.5	11.1 ± 5.1		7.4 ± 4.1		
Trochlear groove (TG)							
1	25.3 ± 10.7	12.1 ± 4.9	7.0 ± 7.0	A	4.1 ± 2.2		A
2	22.0 ± 9.6	8.6 ± 2.4	9.4 ± 6.3		6.0 ± 2.8		
3	13.5 ± 4.1	6.4 ± 3.2	12.5 ± 7.1		7.5 ± 4.1		
Medial ridge (MR)							
1	10.2 ± 7.3	5,1 + 2.2	10.3 ± 6.4		7.2 ± 2.8		
2	11.0 ± 4,3	5,4 + 2.0	9.5 ± 3.5	B	5.4 ± 1.7		B
3	8.6 ± 3.6	4,4 ± 3.4	14.4 ± 7.7		7.1 ± 4.7		
Lateral ridge (LR)							
1	15.2 ± 11.0	5,9 ± 2.5	8.8 ± 4.1		6.4 ± 4.3		
2	13.7 ± 6.8	6,4 ± 3.2	9.7 ± 5.3	AB	5.1 ± 3.4		B
3	10.1 ± 4,4	4,9 ± 2.9	7.4 ± 3.5		4.0 ± 2.6		
Patella (P)							
1	20.0 ± 11.3	7.5 ± 2.9	11.4 ± 4.7	AB	5.4 ± 1.7		AB
2	15.1 ± 4.3	5.6 ± 2.8	11.0 ± 6.6		4.6 ± 2.0		

Data are presented as mean ± s.d. There was no significant variability among sites or regions in the neonate. Regions that varied significantly in the adult are denoted with a unique letter. Properties that varied significantly between adult and neonatal cartilage when averaged across all sites are highlighted in dark gray.

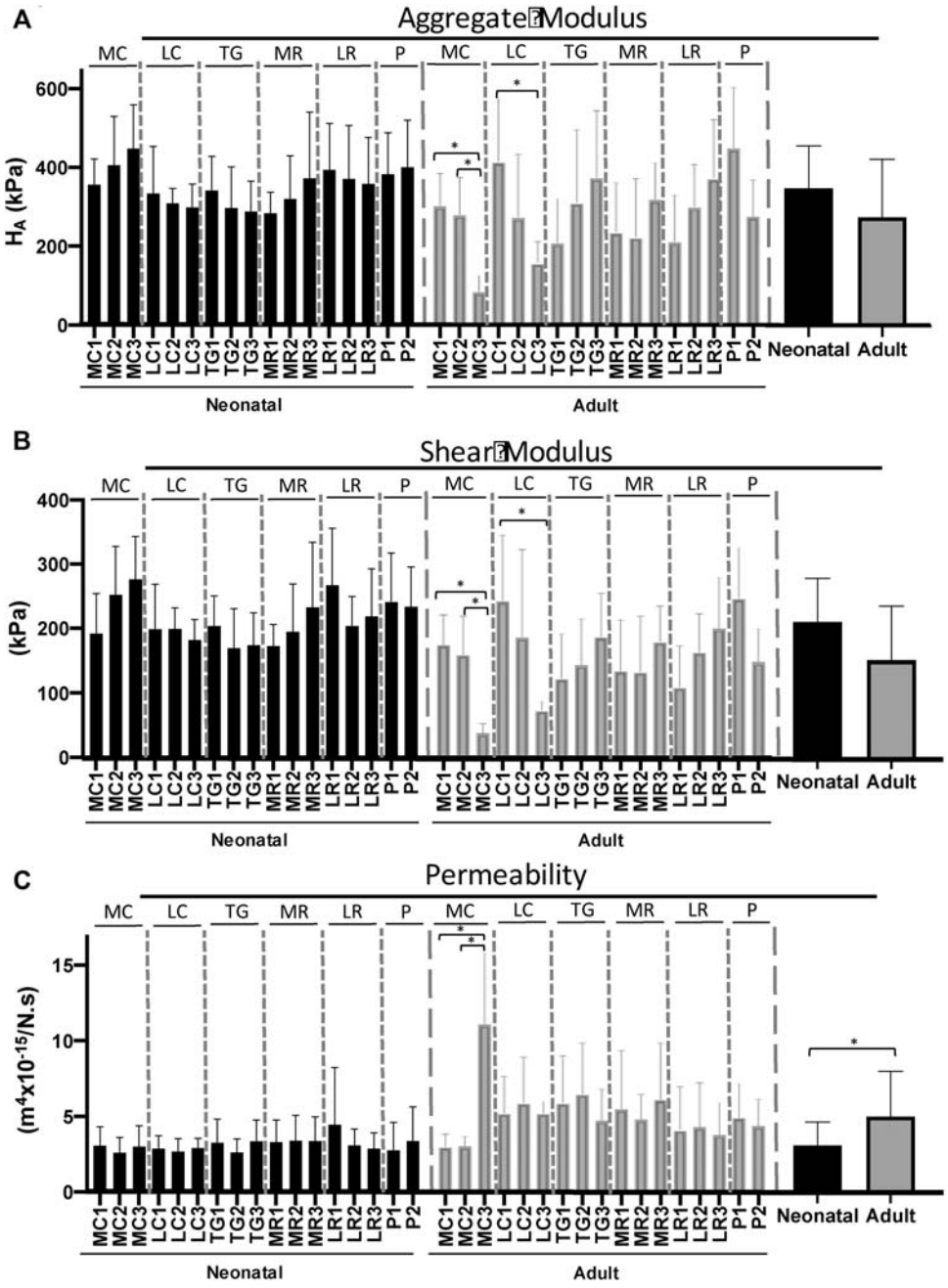

Fig. 6. Characterization of compressive properties at each site within each region and overall average for each age group: neonatal and adult. All values are presented as mean ± s.d. Starred bars (*) represent significant differences among sites within each region as well as between overall averages of each age group. For both aggregate modulus (A) and shear modulus (B), MC1 and MC2 were significantly greater than MC3, and LC1 was significantly greater than LC3 in the adult. (C) Permeability was significantly greater in MC3 than MC1 and MC2 in the adult and varied significantly between the neonate and the adult overall. Compressive property data are available in Table 3.

age groups. In the neonate, however, the TG had significantly higher UTS than the MR and LR. The UTS values measured in the adult stifle in this study are slightly lower (average 5.4 MPa) but comparable with those of a study in which tensile strength was measured at sites on the medial femoral condyle and medial trochlear ridge and found to be 6.7 MPa and 10.7 MPa, respectively [44]. Higher tensile stiffness in neonatal than adult cartilage has been observed in a previous study of the equine metacarpophalangeal joint. This study [42] examined tensile properties and collagen fiber arrangement in neonatal and adult cartilage and found that tensile stiffness correlated with the amount of collagen fibers that were arranged perpendicular to the surface (and thus perpendicular to the axis of tension). In adult cartilage, collagen fibers are primarily aligned parallel to the cartilage surface in the superficial zone and perpendicular to the surface in the deep zone. In neonatal cartilage, this collagen fiber alignment has not fully developed and, as a result, a greater proportion of collagen may have been aligned along the axis of tension, perhaps resulting in a higher measured stiffness [42].

While much of this discussion highlights the statistical differences between neonatal and adult cartilage, there are a number of similarities between cartilages of neonatal and adult horses as well. In spite of those statistical differences, neonatal cartilage possesses mechanical and biochemical properties comparable with adult

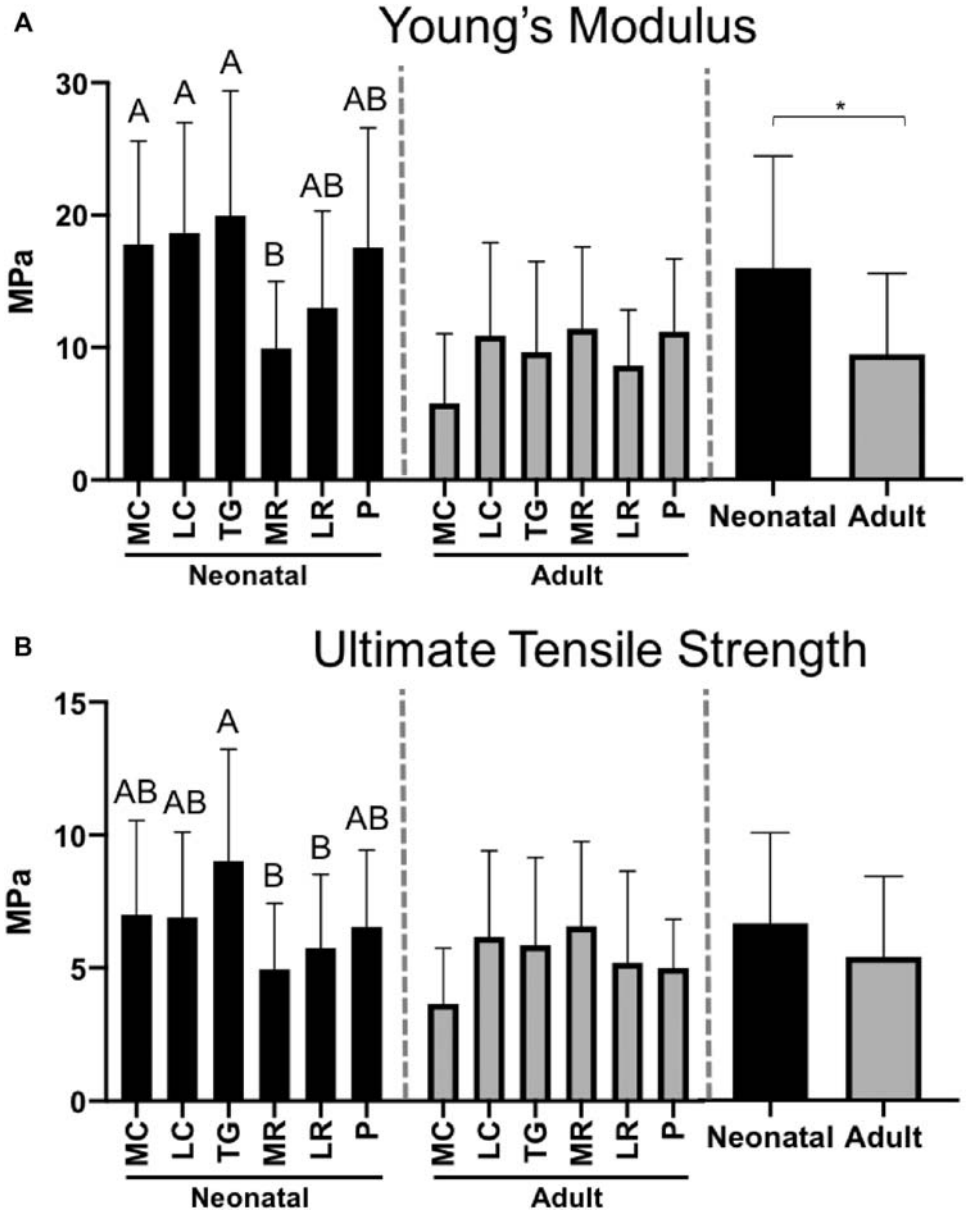

Fig. 7. Characterization of tensile properties within each region and overall average for each age group: neonatal and adult. All values are presented as mean ± s.d. Starred bars (*) represent significant differences between age groups. Regions that do not share the same letter within each age group differ significantly. For both Young's modulus (A) and ultimate tensile strength (UTS), (B) there were significant differences among regions in the neonate but not adult cartilage. Neonatal cartilage had a significantly higher Young's modulus overall as compared with adult cartilage (A) as well.

cartilage, suggesting that neonatal cartilage could withstand the loading forces incurred in the adult. This has implications for allograft techniques that may use a younger donor source for tissue. Good long-term outcome of a graft is undoubtedly a function of whether the graft tissue adequately recapitulates the properties of surrounding native tissue, such that it is able to withstand physiologic loading [45,46]. Furthermore, mismatch between repair tissue and surrounding native tissue results in stress concentrations at the interface between native and repair tissue, which can result in an acceleration of tissue degradation and failure of repair [47]. Using neonatal donor tissue offers the benefit of increased regenerative capacity of tissue from a younger donor source [9,28], which may facilitate lateral integration, while still closely matching properties of host cartilage at time of implantation. Similarities between adult and neonatal tissue properties may also be a consideration in regard to use of neonatal chondrocytes harvested from stifle joint tissue for tissue engineering purposes. It has been demonstrated that neocartilage generated from various locations within a joint possess mechanical properties that corresponded to their tissue of origin, that is chondrocytes harvested from joint regions with higher mechanical properties produced neocartilage with higher mechanical properties than other joint regions [48]. Given that neonatal cartilage possesses properties comparable that of adult cartilage, neonatal chondrocytes may produce tissue engineered neocartilage with comparable properties with adult tissue as well.

Overall, this study characterized multiple locations across the distal femur and patella. As with any topographical study, the resolution of the topographical mapping of the measured properties was limited by the number of sampling sites tested; increasing

the number of sample sites would have allowed for a higher level of understanding of the structure-function relationship between tissue properties and tissue location within the joint. Loading forces experienced by the joint vary in a topographical manner as well. Therefore, to fully understand the relationship between tissue properties and tissue function, concomitant studies to determine forces experienced by articular cartilage during normal loading cycles will also need to be carried out. Additional age groups would further aid in the understanding of how loading influences maturation of articular cartilage, and how this maturation process manifests in regards to biochemical and biomechanical properties of the tissue. Another limitation of this study was the inability to acquire full-thickness neonatal articular cartilage samples, which prevented comparison with the thickness of the adult cartilage, as well as probing any relationships between cartilage thickness and function in the neonate. However, while trimming may have excluded a small portion of deeper neonatal cartilage, the lack of distinct articular cartilage zonal variation in neonates likely reduced the variability this technique could have caused in the results of other assays [49]. Another major limitation of this study was the heterogeneity of the patient population used in this study, which undoubtedly contributed to the large amount of variability in biochemical and biomechanical results. This study specifically compared neonatal and adult cartilage as neonatal cartilage and chondrocytes may serve as an ideal donor source for allografts or chondrocytes for tissue engineering strategies aimed at repair of damaged articular cartilage in the adult equine athlete. The results of this study, therefore, can be used in the establishment of design criteria for future engineered equine articular cartilage products as well as aid in assessment of the performance of engineered tissues in both *in vitro* and *in vivo* contexts.

5. Conclusion

This study provides qualitative and quantitative properties of native articular cartilage from the stifle of both neonatal and skeletally mature adult horses. This study represents the first time neonatal articular cartilage was comprehensively and quantitatively examined from the stifle and compared with adult cartilage in a head-to-head manner. The examination revealed significant differences as well as similarities in morphological, histologic, biochemical, and biomechanical properties among sites within joint regions as well as age-related differences between neonatal and adult cartilage. An understanding of these location and age-related differences in properties between the therapeutic target cartilage (i.e., adult cartilage) as well as potential donor cartilage (i.e., neonatal cartilage) could aid in selection of optimal harvest sites within a donor joint as well as evaluation of the success of the grafted cells or tissues within the host. In addition, this work furthers the knowledge of cartilage tissue physiology and structure-function relationships.

Acknowledgments

This project was supported in part by funds provided by the National Center for Advancing Translational Sciences and National Institutes of Health, through grant number UL1 TR001860 and linked award TL1 TR001861. JML was also in part funded by a National Science Foundation Graduate Research Fellowship (Grant No. 1650042).

References

[1] Singer ER, Barnes J, Saxby F, Murray JK. Injuries in the event horse: training versus competition. Vet J 2008;175:76–81.
[2] Jiménez G, Cobo-Molinos J, Antich C, López-Ruiz E. Osteoarthritis: trauma vs disease. osteochondral tissue engineering, 1059. Cham: Springer International Publishing; 2018. p. 63–83.
[3] De Lasalle J, Alexander K, Olive J, Laverty S. Comparisons among radiography, ultrasonography and computed tomography for ex vivo characterization of stifle osteoarthritis in the horse. Vet Radiol Ultrasound 2016;57:489–501.
[4] Huang BJ, Hu JC, Athanasiou KA. Cell-based tissue engineering strategies used in the clinical repair of articular cartilage. Biomaterials 2016;98:1–22.
[5] Makris EA, Gomoll AH, Malizos KN, Hu JC, Athanasiou KA. Repair and tissue engineering techniquesfor articular cartilage. Nature Publishing Group; 2014. p. 1–14.
[6] Cokelaere S, Malda J, van Weeren R. Cartilage defect repair in horses: current strategies and recent developments in regenerative medicine of the equine joint with emphasis on the surgical approach. Vet J 2016;214:61–71.
[7] Ortved KF, Nixon AJ. Cell-based cartilage repair strategies in the horse. Vet J 2016;208:1–12.
[8] McIlwraith CW, Fortier LA, Frisbie DD, Nixon AJ. Equine models of articular cartilage repair. Cartilage 2011;2:317–26.
[9] Smeriglio P, Lai JH, Dhulipala L, Behn AW, Goodman SB, Smith RL, et al. Comparative potential of juvenile and adult human articular chondrocytes for cartilage tissue formation in three-dimensional biomimetic hydrogels. Tissue Eng A 2015;21:147–55.
[10] Brama PAJ, Holopainen J, van Weeren PR, Firth EC, Helminen HJ, Hyttinen MM. Influence of exercise and joint topography on depth-related spatial distribution of proteoglycan and collagen content in immature equine articular cartilage. Equine Vet J 2009;41:557–63.
[11] Brama PAP, Tekoppele JMJ, Bank RAR, van Weeren PRP, Barneveld AA. Influence of different exercise levels and age on the biochemical characteristics of immature equine articular cartilage. Audio, Transactions of the IRE Professional Group on 1999:55–61.
[12] Brama PAJ, Holopainen J, van Weeren PR, Firth EC, Helminen HJ, Hyttinen MM. Effect of loading on the organization of the collagen fibril network in juvenile equine articular cartilage. J Orthop Res 2009;27:1226–34.
[13] Brama PAJ, Tekoppele JM, Bank RA, Karssenberg D, Barneveld A, van Weeren PR. Topographical mapping of biochemical properties of articular cartilage in the equine fetlock joint. Equine Vet J 2000;32:19–26.
[14] Hyttinen MM, Holopainen J, René van Weeren P, Firth EC, Helminen HJ, Brama PAJ. Changes in collagen fibril network organization and proteoglycan distribution in equine articular cartilage during maturation and growth. J Anat 2009;215:584–91.
[15] Holopainen JT, Brama PAJ, Halmesmäki E, Harjula T, Tuukkanen J, van Weeren PR, et al. Changes in subchondral bone mineral density and collagen matrix organization in growing horses. Bone 2008;43:1108–14.
[16] van der Harst MR, van de Lest CHA, DeGroot J, Kiers GH, Brama PAJ, van Weeren PR. Study of cartilage and bone layers of the bearing surface of the equine metacarpophalangeal joint relative to different timescales of maturation. Equine Vet J 2005;37:200–6.
[17] Brommer H, Brama PAJ, Laasanen MS, Helminen HJ, van Weeren PR, Jurvelin JS. Functional adaptation of articular cartilage from birth to maturity under the influence of loading: a biomechanical analysis. Equine Vet J 2005;37:148–54.
[18] Weeren PR, Firth EC, Brommer H, Hyttinen MM, Helminen HJ, ROGERS CW, et al. Early exercise advances the maturation of glycosaminoglycans and collagen in the extracellular matrix of articular cartilage in the horse. Equine Vet J 2010;40:128–35.
[19] Brama P, Tekoppele JM, Bank RA, Barneveld A, van Weeren PR. Functional adaptation of equine articular cartilage: the formation of regional biochemical characteristics up to age one year. Equine Vet J 2000;32:217–21.
[20] Vachon AM, Keeley FW, McIlwraith CW, Chapman P. Biochemical analysis of normal articular cartilage in horses. Am J Vet Res 1990;51:1905–11.
[21] Palmer JL, Bertone AL, Malemud CJ, Carter BG, Papay RS, Mansour J. Site-specific proteoglycan characteristics of third carpal articular cartilage in exercised and nonexercised horses. Am J Vet Res 1995;56:1570–6.
[22] Palmer JL, Bertone AL, Malemud CJ, Mansour J. Biochemical and biomechanical alterations in equine articular cartilage following an experimentally-induced synovitis. Osteoarthritis Cartilage 1996;4:127–37.
[23] Murray RC, DeBowes RM, Gaughan EM, Zhu CF, Athanasiou KA. The effects of intra-articular methylprednisolone and exercise on the mechanical properties of articular cartilage in the horse. Osteoarthritis Cartilage 1998;6:106–14.
[24] Murray RC, DeBowes RM, Gaughan EM, Mosier DE, Athanasiou KA. Variations in the biomechanical properties of articular cartilage of the Midcarpal joint of normal horses. Vet Comp Orthop Traumatol 1995;8:11–8.
[25] Murray RC, Zhu CF, Goodship AE, Lakhani KH, Agrawal CM, Athanasiou KA. Exercise affects the mechanical properties and histological appearance of equine articular cartilage. J Orthop Res 1999;17:725–31.
[26] O'Leary SA, White JL, Hu JC, Athanasiou KA. Biochemical and biomechanical characterisation of equine cervical facet joint cartilage. Equine Vet J 2018;50:800–8.
[27] Changoor A, Hurtig MB, Runciman RJ, Quesnel AJ, Dickey JP, Lowerison M. Mapping of donor and recipient site properties for osteochondral graft reconstruction of subchondral cystic lesions in the equine stifle joint. Equine Vet J 2006:1–7.
[28] Yanke AB, Tilton AK, Wetters NG, Merkow DB, Cole BJ. DeNovo NT particulated juvenile cartilage implant. Sports Med Arthrosc Rev 2015;23:125–9.

[29] Taylor SEB, Lee J, Smeriglio P, Razzaque A, Smith RL, Dragoo JL, et al. Identification of human juvenile chondrocyte-specific factors that stimulate stem cell growth. Tissue Eng Part A 2016;22:645–53.
[30] Athanasiou KA, Agarwal A, Muffoletto A, Dzida FJ, Constantinides G, Clem M. Biomechanical properties of hip cartilage in experimental animal models. Clin Orthop Relat Res 1995:254–66.
[31] Cissell DD, Link JM, Hu JC, Athanasiou KA. A modified hydroxyproline assay based on hydrochloric acid in ehrlich's solution accurately measures tissue collagen content. Tissue Eng C Methods 2017;23:243–50.
[32] Bank RA, Beekman B, Verzijl N, de Roos JA, Sakkee AN, Tekoppele JM. Sensitive fluorimetric quantitation of pyridinium and pentosidine crosslinks in biological samples in a single high-performance liquid chromatographic run. J Chromatogr B Biomed Sci Appl 1997;703:37–44.
[33] Bibbiani C, Tongiani R, Viola-Magni MI. Quantitative determination of the amount of DNA per nucleus by interference microscopy. J Cell Biol 1969;42:444–51.
[34] Ionescu LC, Lee GC, Garcia GH, Zachry TL, Shah RP, Sennett BJ, et al. Maturation state-dependent alterations in meniscus integration: implications for scaffold design and tissue engineering. Tissue Eng Part A 2011;17:193–204.
[35] Wong M, Carter DR. Articular cartilage functional histomorphology and mechanobiology: a research perspective. Bone 2003;33:1–13.
[36] Halley SE, Bey MJ, Haladik JA, Lavagnino M, Arnoczky SP. Three dimensional, radiosteriometric analysis (RSA) of equine stifle kinematics and articular surface contact: a cadaveric study. Equine Vet J 2013;46:364–9.
[37] Adrian AM, Barrett MF, Werpy NM, Kawcak CE, Chapman PL, Goodrich LR. A comparison of arthroscopy to ultrasonography for identification of pathology of the equine stifle. Equine Vet J 2016;49:314–21.
[38] Fowlie JG, Arnoczky SP, Stick JA, Pease AP. Meniscal translocation and deformation throughout the range of motion of the equine stifle joint: an in vitro cadaveric study. Equine Vet J 2010;43:259–64.
[39] Gillooly JF, Hein A, Damiani R. Nuclear DNA content varies with cell size across human cell types. Cold Spring Harb Perspect Biol 2015;7. a019091–27.
[40] Poole CA, Matsuoka A, Schofield JR. Chondrons from articular cartilage. III. Morphologic changes in the cellular microenvironment of chondrons isolated from osteoarthritic cartilage. Arthritis Rheum 1991;34:22–35.
[41] D'Lima DD, Hashimoto S, Chen PC, Colwell CW, Lotz MK. Impact of mechanical trauma on matrix and cells. Clin Orthop Relat Res 2001;391:S90–9.
[42] Oinas J, Ronkainen AP, Rieppo L, Finnilä MAJ, Iivarinen JT, van Weeren PR, et al. Composition, structure and tensile biomechanical properties of equine articular cartilage during growth and maturation. Sci Rep 2018;8:1–12.
[43] Athanasiou KA, Darling EM, Hu JC, DuRaine GD, Reddi AH. Articular cartilage. CRC Press; 2017.
[44] Lewis CW, Williamson AK, Chen AC, Bae WC, Temple MM, Wong WV, et al. Evaluation of subchondral bone mineral density associated with articular cartilage structure and integrity in healthy equine joints with different functional demands. Am J Vet Res 2005;66:1823–9.
[45] Koh Y-G, Lee J-A, Kim YS, Lee HY, Kim HJ, Kang K-T. Optimal mechanical properties of a scaffold for cartilage regeneration using finite element analysis. J Tissue Eng 2019;10. 2041731419832133.
[46] Bowland P, Ingham E, Jennings L, Fisher J. Review of the biomechanics and biotribology of osteochondral grafts used for surgical interventions in the knee. Proc Inst Mech Eng H 2015;229:879–88.
[47] Kock NB, Smolders JMH, van Susante JLC, Buma P, van Kampen A, Verdonschot N. A cadaveric analysis of contact stress restoration after osteochondral transplantation of a cylindrical cartilage defect. Knee Surg Sports Traumatol Arthrosc 2008;16:461–8.
[48] Paschos NK, Makris EA, Hu JC, Athanasiou KA. Topographic variations in biomechanical and biochemical properties in the ankle joint: an in vitro Bovine study evaluating native and engineered cartilage. Arthroscopy 2014;30:1317–26.
[49] Cluzel C, Blond L, Fontaine P, Olive J, Laverty S. Foetal and postnatal equine articular cartilage development: magnetic resonance imaging and polarised light microscopy. Eur Cell Mater 2013;26:33–48.